

Structure–Activity Relationship and Rational Design of 3,4-Dephostatin Derivatives as Protein Tyrosine Phosphatase Inhibitors

Takumi Watanabe,^a Takayuki Suzuki,^b Yoji Umezawa,^a Tomio Takeuchi,^a Masami Otsuka^c and Kazuo Umezawa^{b,*}

^aInstitute of Microbial Chemistry, 3-14-23 Kamiosaki, Shinagawa-ku, Tokyo 141-0021, Japan

^bDepartment of Applied Chemistry, Faculty of Science and Technology, Keio University, 3-14-1 Hiyoshi, Kohoku-ku, Yokohama 223-0061, Japan

^cFaculty of Pharmaceutical Sciences, Kumamoto University, 5-1 Oe-Honmachi, Kumamoto 862-0973, Japan

Received 5 November 1999; accepted 6 December 1999

Abstract—Several alkyl- and *O*-methylated-3,4-dephostatin were synthesized and evaluated for their inhibitory activity toward protein tyrosine phosphatase. Alkyl chains with a length up to that of the pentyl group gave tolerable inhibition, whereas methylation of hydroxyl groups resulted in a decrease in the activity. Based on the structure–activity relationship and X-ray crystallographic analysis of C215S PTP1B–phosphotyrosine containing peptide complex, the mode of binding of 3,4-dephostatins to the active site was speculated with the aid of calculation. Several hydrogen bonds and CH/ π interactions were suggested to be important for inhibition of PTPase. A novel nitroso-free methoxime compound was designed so that all the attractive interactions were maintained. The methoxime compound was synthesized and shown to inhibit PTP1B. © 2000 Elsevier Science Ltd. All rights reserved.

Many biological phenomena including cellular proliferation, differentiation, and apoptosis are controlled by intracellular signal transduction initiated by external stimuli. Various proteins and low-molecular-weight compounds take part in these signaling systems. Overexpression of the specific signal proteins often causes diseases such as neoplasia and diabetes mellitus. Consequently, inhibitors of the enzymes involved in such overexpression are considered to be candidates for novel chemotherapeutic agents.

Protein-tyrosine kinases (PTKases) are typical signaling molecules for cell growth, differentiation, and transformation. Therefore, protein-tyrosine phosphatases (PTPases), enzymes having the opposite action, should be equally important as PTKases for the regulation of these phenotypic changes.¹ However, the lack of potent and selective PTPase inhibitor has retarded the further clarification of the physiological function of PTPases. Currently, only sodium vanadate, which also inhibits Ca²⁺ and K⁺-dependent ATPase, is frequently used as an inhibitor of PTPases.

In 1993, our group reported the isolation and structure determination of dephostatin (**1**) (Fig. 1)^{2,3} as the first naturally occurring selective PTPase inhibitor. Dephostatin has

unique structural characteristics, i.e. a hydroquinone skeleton with an *N*-methyl-*N*-nitrosoamino moiety. This compound inhibits CD45 (receptor type PTPase) activity comparably to sodium vanadate, and does not inhibit serine/threonine phosphatases such as PP2A and PP2B. However, an adequate amount of dephostatin cannot be obtained from natural sources because of the low productivity of microorganisms. Therefore, we accomplished the first total synthesis of dephostatin.⁴ However, the intrinsic lability of this compound hampered the practical application of it to biological studies. To overcome this drawback, we started to search for stable yet potent dephostatin analogs. Substitution of the nitroso moiety to a carboxamide or sulfonamide resulted in complete loss of activity. The number and position of the phenolic hydroxyl groups were also found to be important, for dephostatin lost its activity upon the methylation or removal of hydroxyl groups. Among the synthesized regio-isomers of dephostatin,

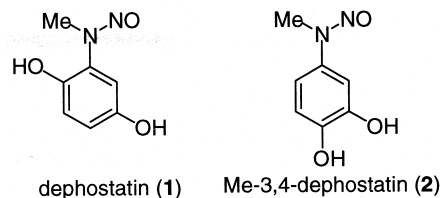


Figure 1. The structure of dephostatin and Me-3,4-dephostatin.

Keywords: enzyme inhibitors; structure–activity; molecular design; molecular modeling/mechanics.

* Corresponding author; e-mail: umezawa@apple.keio.ac.jp

only the 3,4-dihydroxy isomer of dephostatin **2** (named Me-3,4-dephostatin for convenience) inhibited the PTPase activity of CD45.⁵ Me-3,4-dephostatin competes with the substrate,⁶ and it is noteworthy that Me-3,4-dephostatin is at least 10 times more stable than dephostatin in media used for animal cell cultures.⁶

Using Me-3,4-dephostatin, we demonstrated that PTPase participates in nerve cell differentiation. Me-3,4-dephostatin enhanced NGF or EGF-induced differentiation of rat pheochromocytoma PC12 cells, possibly by sustaining the downstream MAP kinase activity.⁷ PTPases such as PTP1B^{8,9} and LAR^{10,11} are known to antagonize the effects of insulin. PTP1B-knock out mice showed increased sensitivity to insulin.¹² Therefore, PTPase inhibitors may be developed in the future as new therapeutics for neural injury, neural diseases including Alzheimer's and Parkinson's diseases, and diabetes mellitus.

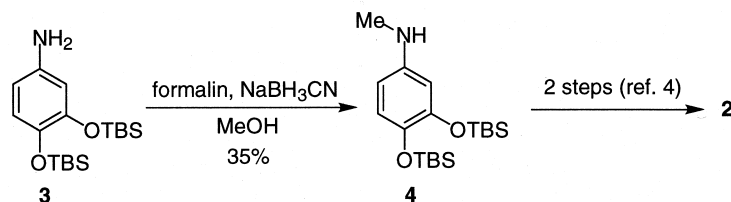
Most of the PTPase inhibitors so far reported were rationally designed based on the structure of peptides containing phosphotyrosine. Phosphotyrosine mimetics having a nonhydrolyzable substituent such as phosphonate instead of phosphate ester were frequently utilized to develop potent and selective PTPase inhibitors. 4-Phosphono(difluoromethyl)-L-phenylalanine (F₂Pmp) derivatives¹³ were synthesized as phosphotyrosine mimetics that can bind to the SH2 domains of various proteins such as phosphatidylinositol (PI) 3-kinase, Src and Grb2.^{14,15} F₂Pmp works as a PTPase inhibitor by taking the place of the phosphotyrosine residue of the peptidyl substrate. The resulting peptides act as highly potent and selective PTPase inhibitors. Mechanistic aspects of PTPase inhibitory activity of F₂Pmp-related compounds were thoroughly investigated.^{16,17} In these studies, the fluorine atoms of the phosphonate moiety were shown to participate in hydrogen bonding with the active site of PTPases. Many kinds of F₂Pmp-related substances were also synthesized.^{18,19} Besides F₂Pmp, various phosphotyrosine mimetics including *O*-malonyl tyrosine derivatives (OMT and FOMT),^{20,21} a thiophosphorylated tyrosine derivative,²² cinnamate derivatives,²³ and a salicylic acid carboxymethyl ether derivative²⁴ have been reported. In addition, some tyrosine-based compounds inhibit PTPase activity by covalent bond formation.^{25,26} Naturally occurring PTPase inhibitors such as RK-682,²⁷ aporphine alkaloids including anonaine and nornuciferine,²⁸ pulchellalactam,²⁹ and phosphatoquinones A and B³⁰ have also been reported. PTPase inhibitors having hitherto unknown structural characteristics were discovered by the combinatorial synthesis approach.³¹ Although various PTPase inhibitors as above have been reported, sodium vanadate is still the most widely used to inhibit PTPases in biological studies.

Recently, X-ray crystallographic analyses of many enzymes and enzyme–inhibitor complexes have been reported, and it is often possible to develop more potent inhibitors by rational design based on the mechanistic interpretation. X-Ray crystallography of some PTPases has already been reported. Among them, the 3-D structure of C215S PTP1B complexed with an *O*-phosphotyrosine should be useful for speculating on the inhibition of PTPase by low-molecular-weight compounds.³² This mutated PTP1B loses its catalytic activity without a change in the structure of the active site. In this paper, the roles of the *N*-alkyl moiety and the phenolic hydroxyl groups of 3,4-dephostatin in its PTPase inhibitory activity are described. Then, based on the structure activity relationship and the 3-D structure of PTP1B–*O*-phosphotyrosine complex,³² the most favorable interaction of 3,4-dephostatin with the enzyme is calculated computationally considering hydrogen bondings and CH/ π interactions.^{33,34} Finally, structurally novel and potent PTPase inhibitors are designed and synthesized based on such calculations.

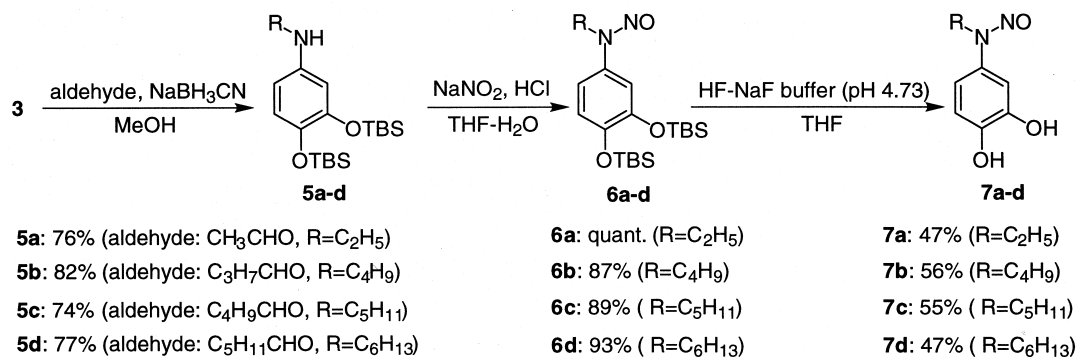
Synthesis of 3,4-Dephostatin Analogs

Previously we reported the synthesis of Me-3,4-dephostatin⁵ starting from 3,4-dimethoxyaniline. A disadvantage of this route is that the step of trifluoroacetamide hydrolysis is often accompanied by the simultaneous removal of the silyl groups. The resulting fully deprotected product was too unstable to isolate. Therefore, we looked for a more efficient route for preparation of Me-3,4-dephostatin. According to Wang's synthesis of dephostatin,³⁵ reductive amination (HCHO and NaBH₃CN) of the known aniline derivative **3**³⁶ gave monomethylated product **4**. Although the yield of this step was moderate, the unreacted starting material could be recovered and reused. The resulting compound **4** was identical to an intermediate of the previously reported synthesis,⁵ from which the desired Me-3,4-dephostatin can be obtained in two steps with no difficulty (Scheme 1).

Other alkyl groups can easily be introduced by using corresponding aldehydes. Succeeding nitrosation and deprotection were accomplished by reported procedure to give the requisite analogs. In this study, ethyl, butyl, pentyl, and hexyl groups were introduced to investigate the relationships between the bulkiness of the alkyl moiety and the enzyme inhibitory activity (Scheme 2). Methyl ether derivatives of Me-3,4-dephostatin (**14a** and **14b**) were also synthesized by the above reductive amination from suitable starting materials. The dimethoxy compound **16** was obtained by a one step procedure (Scheme 3).



Scheme 1. Improved synthesis of Me-3,4-dephostatin.



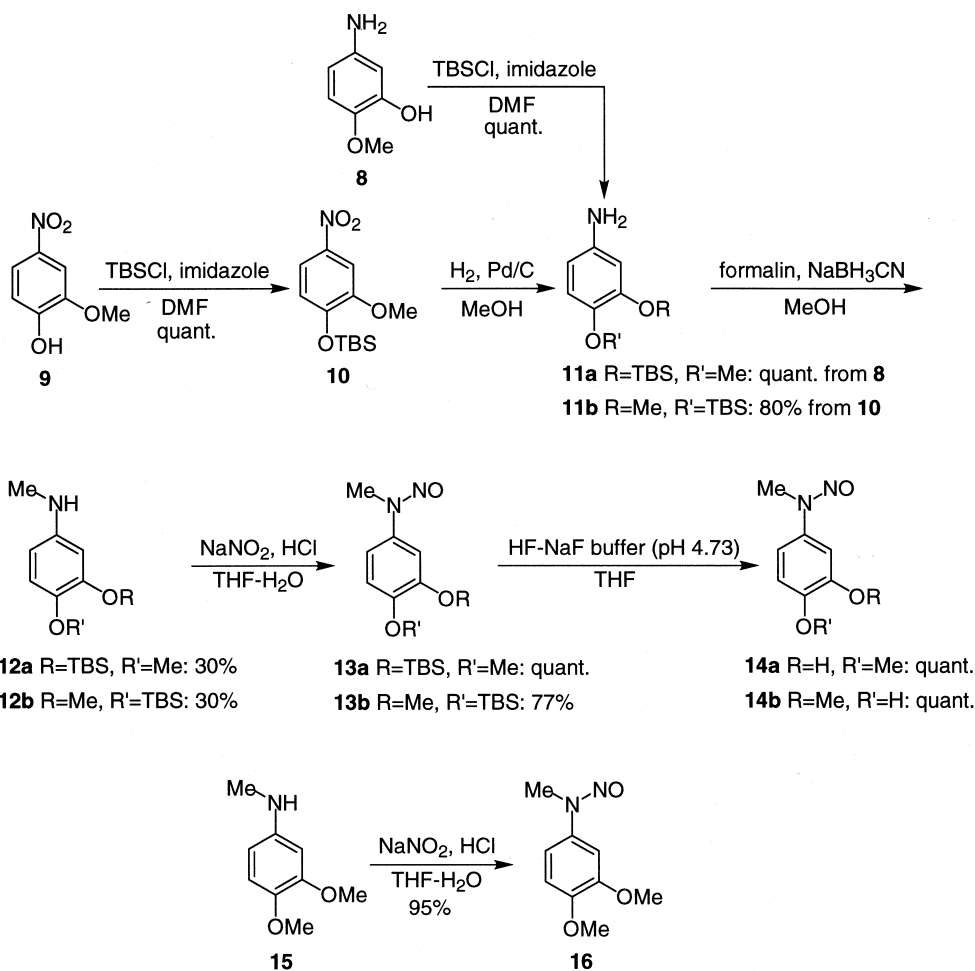
Scheme 2. Synthesis of alkyl-3,4-dephostatin analogs.

Inhibition of PTPase by 3,4-Dephostatin Derivatives

The PTPase inhibitory activity of the synthesized 3,4-dephostatin analogs was examined. In our previous study,⁴ we used crude CD45 prepared from Jurkat cell membranes as the enzyme source. In this study, commercially available PTP1B was used because the 3-D structure of PTP1B has been elucidated. This enzyme is also known to be involved in the regulation of insulin receptor activity. The purified enzyme was used with *p*-nitrophenyl phosphate as the

substrate. After the reaction, the hydrolysis product, *p*-nitrophenol, was quantified by a colorimetric method.

Inhibition of PTPases by the various 3,4-dephostatin derivatives is shown in Table 1. The length of the alkyl chain influenced the inhibitory activity. Up to the pentyl chain, inhibition comparable to that of Me-3,4-dephostatin was observed. However, introduction of hexyl group decreased the inhibitory activity. Hydroxyl groups were shown to be essential for the inhibitory activity. Blocking



Scheme 3. Synthesis of methylated Me-3,4-dephostatin analogs.

Table 1. PTP1B inhibition by 3,4-dephostatin analogs

Compound	IC ₅₀ (μg/mL)
2	0.52
7a	0.58
7b	0.60
7c	0.30
7d	1.52
14a	>100
14b	48
16	>100
Sodium vanadate	0.30

of the hydroxyl groups by methyl group apparently decreased the activity. These results suggest that both hydroxyl groups of 3,4-dephostatin participate in the interaction with PTP1B, presumably by involvement in hydrogen bonding, as discussed later.

Computational Analysis of 3,4-Dephostatin–PTPase Interaction

Based on mutated PTP1B–phosphotyrosine complex,³² the most favorable interaction between PTP1B and Me-3,4-dephostatin derivatives was obtained by calculation using the CVFF force field parameter. In protein–ligand complexes, ionic interaction, hydrogen bonding, and hydrophobic effects are considered to be the major attractive non-covalent interactions. In particular, hydrogen bonding and ionic interaction have been widely considered to be involved in molecular recognition, whereas the hydrophobic effect is a far more vague concept.

Recently, CH/ π interaction was revealed to have a critical role in protein–ligand complexation and folding of proteins. CH/ π interaction is a hydrogen-bond-like weak attractive force observed between the CH hydrogen and the π electron system. The CH hydrogens and π rings in biomolecules often create a large network of CH/ π interactions. To estimate the contribution of CH/ π interaction to PTP1B and 3,4-dephostatin related compounds, the CHPI program was used.³⁷ This program was written in order to search for

the short contacts between the CH groups and π systems in protein structures registered in the protein data bank (PDB). This program detects XH/ π interaction (X=C, N, O and S) bases on bond length and angle parameters.

The crystal structure of C215S PTP1B–*O*-phosphotyrosine complex was recently reported.³² Firstly, Me-3,4-dephostatin was superimposed to *O*-phosphotyrosine in the C215S PTP1B–substrate complex so that the anilinic portion of Me-3,4-dephostatin overlapped with the phenolic part of *O*-phosphotyrosine, as shown in Fig. 2. Then, the energetically minimized structure was searched for, in which all of the coordinates of atoms of PTP1B more than 7 Å apart from the ligand were fixed. The motion of atoms between 5 and 7 Å was set to be movable within limit by the software, whereas that of atoms less than 5 Å distant was fully movable. Fig. 3 shows the presumed binding mode between PTP1B and Me-3,4-dephostatin. In the optimized structure, the oxygen atom of the nitroso moiety tightly interacted with the guanidium residue of R 221 by hydrogen bonding. A similar interaction was observed in phosphate oxygen of phosphotyrosine–C215S PTP1B complex. No important interaction was observed between the anilinic nitrogen atom and the active site.

The phenolic hydroxyl group at the 3-position formed a hydrogen bond with the side chain of glutamine. Loss of the PTPase inhibitory activity of 3-*O*-methylated Me-3,4-dephostatin clearly indicated the necessity of the hydroxyl group. On the other hand, the 4-OH group seems not to be responsible for binding to the active site, and is presumed to participate only in intramolecular hydrogen bonding. However, since 4-*O*-methylation of Me-3,4-dephostatin resulted in only weak inhibitory activity, the electronic structure of 3,4-dephostatin may also be important for the inhibition of PTPase. In fact, monohydroxy dephostatin analog, 3-hydroxy-*N*-methyl-*N*-nitrosoaniline, showed no PTPase inhibitory activity.⁵

The methyl group on the nitrosamine moiety was oriented inside the active site pocket. The active site pocket seems to be deep enough to accommodate longer alkyl chains. Fig. 4 shows the result of calculation of

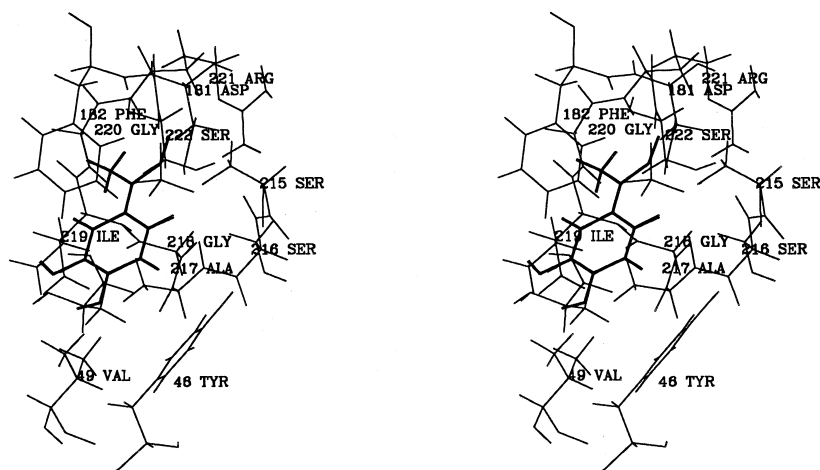


Figure 2. Superimposition of Me-3,4-dephostatin to *O*-phosphotyrosine in the PTP1B–substrate complex. (Me-3,4-dephostatin is shown by bold lines, and *O*-phosphotyrosine by plain lines. The phenolic moiety of *O*-phosphotyrosine is overlapped with the portion of Me-3,4-dephostatin.)

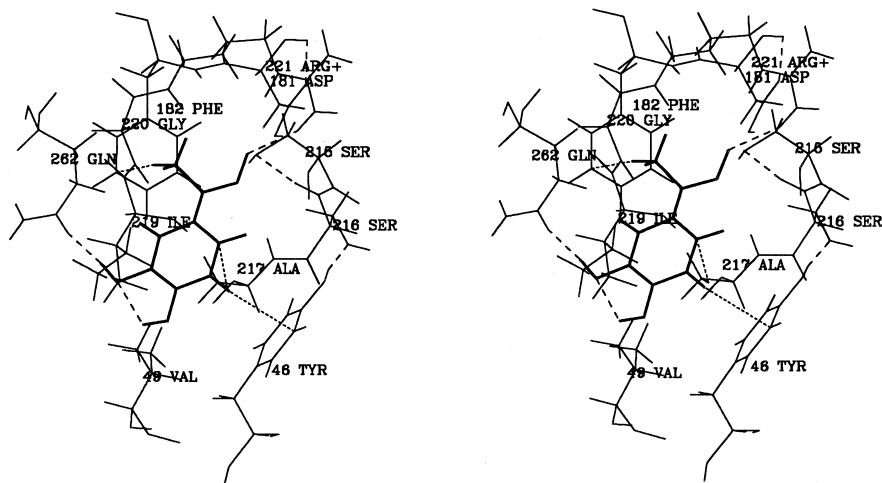


Figure 3. Stereoview of proposed binding mode between Me-3,4-dephostatin and PTP1B. (CH/ π interactions are shown by dotted lines; and hydrogen bonding by broken lines.)

PTP1B–pentyl-3,4-dephostatin superimposition. The pentyl derivative showed potent inhibitory activity, but the hexyl derivative apparently showed weaker activity. The long alkyl chain participates in the CH/ π with F 182, but a larger alkyl group cannot be accommodated without weakening the essential hydrogen bondings.

Design and Synthesis of New PTPase Inhibitors

According to the possible interaction mentioned above, new PTPase inhibitors were designed and synthesized. Since Et-3,4-dephostatin **7a** was stable compared with Me-3,4-dephostatin, it was used in a recent biological study in our group for the development of new antidiabetic agents. However, Et-3,4-dephostatin turned out to be weakly mutagenic in the *Salmonella* mutation assay. The mutagenicity should come from its nitrosamine moiety. To eliminate this disadvantage, we designed novel PTPase inhibitors having no nitrosamine structure.

Firstly, the tetrazole derivative (**20**) depicted in Scheme 4 was designed. The N–N=N bondings on the tetrazole ring were expected to be a good substitute for the N–N=O bondings. As shown in Scheme 4, the amino group of **17**³⁸ was converted into an isocyano group by formylation and subsequent dehydration using triphosgene.³⁹ The tetrazole ring was constructed by 1,3-dipolar cycloaddition of sodium azide to the isocyano group⁴⁰ in the presence of ammonium chloride. In this step, concomitant deacetylation occurred to afford the desired tetrazole derivative.

However, **20** showed no activity possibly because of an unexpected geometrical mismatch between the N–N=N structure of tetrazole and the N–N=O structure of the nitrosamine. Differences in the bond angles of the five-membered ring and the open structure would affect their activity. In fact, simple superimposition of the tetrazole derivative into the active site of PTP1B showed that the N=N bond of tetrazole largely deviated from the N=O bond of Me-3,4-dephostatin (data not shown).

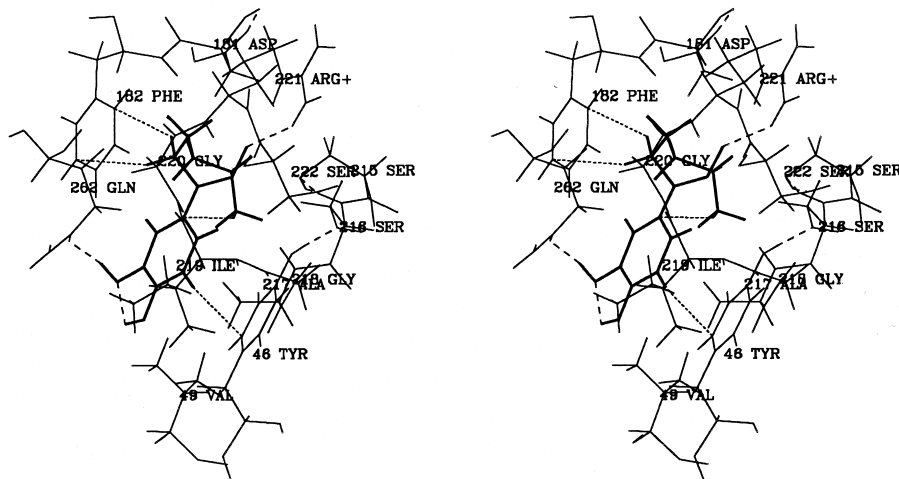
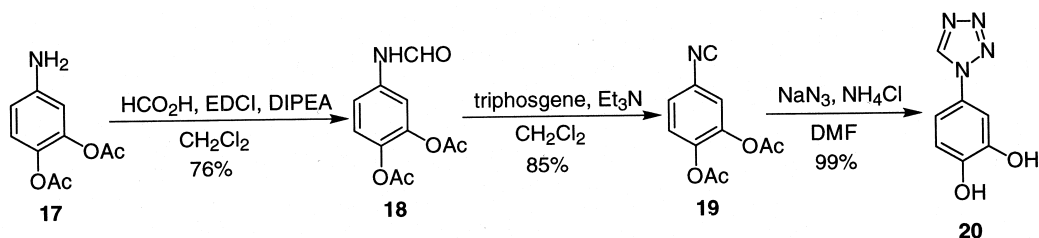
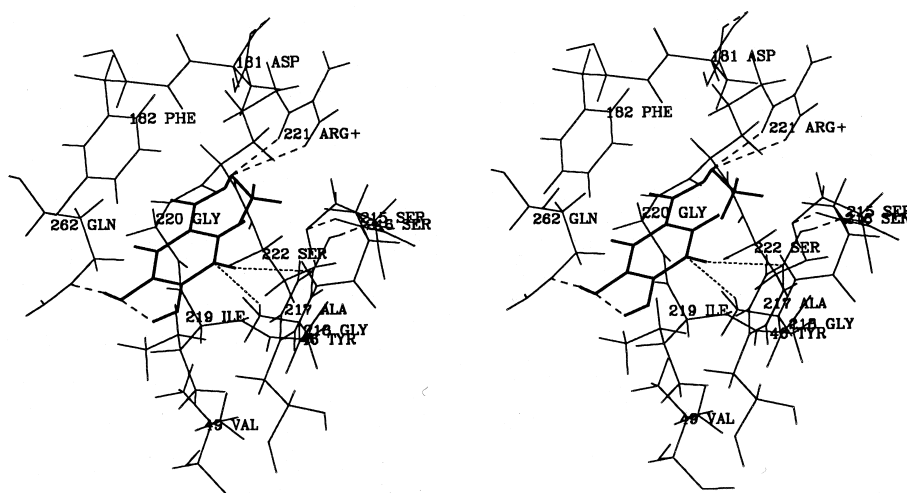


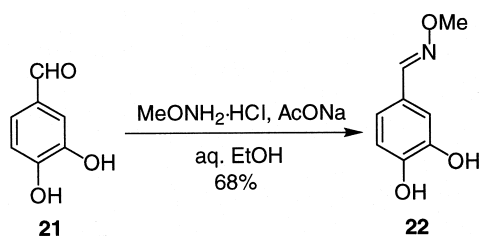
Figure 4. Stereoview of proposed binding mode between pentyl-3,4-dephostatin and the active site of PTP1B. (CH/ π interactions are shown by dotted lines; and hydrogen bonding by broken lines.)



Scheme 4. Synthesis of tetrazole derivative.

Figure 5. Stereoview of expected binding mode between methoxime **22** and PTP1B. (CH/π interactions are shown by dotted lines; and hydrogen bonding by broken lines.)

Then, we tried to design open chain alcoximes as the next candidates. Fig. 5 shows the hypothesized mode of binding of the designed methoxime compound (**22**). Both the N–N=O bond of Me-3,4 dephostatin and the C=N–O bond of methoxime are considered to have the character of a partial double bond. Thus, each nitrogen–oxygen bond should have similar electronic nature. Moreover, Fig. 1 showed that the nitrogen atom attached to the benzene ring of Me-3,4-dephostatin has no interaction with the surrounding structure. Therefore, converting this nitrogen atom to a carbon atom would likely be tolerable. The oxygen atom of the methoxime moiety would be expected to participate in the hydrogen bonding with the arginine side chain. The distance from oxygen to arginine is longer than in the case of 3,4-dephostatin, which may come from the steric influence of the methyl group. However, their bidentate binding would be expected to compensate for the disadvantage in distance.



Scheme 5. Synthesis of methoxime compound.

Condensation of **21** and methoxyamine hydrochloride in the presence of sodium acetate gave the methoxime **22** (Scheme 5).⁴¹ The geometry of the resulting methoxime was unequivocally confirmed as *E* by X-ray crystallographic analysis, as shown in the Experimental section. As expected, the methoxime inhibited PTP1B phosphatase with an IC_{50} of 2.9 $\mu\text{g/mL}$, which was only five times higher than that of Me-3,4-dephostatin (Table 2). The decrease in activity may have come from the loss of CH/π interaction between the methoxime group and the active site. There is enough room for further elongation and functionalization of the methoxy moiety of this compound. Therefore, suitable designing of the alkoxy moiety to give an additional affinity for the enzyme active site should potentiate its PTPase inhibitory activity.

Conclusion

The role of the alkyl group on the nitrosamine moiety and that of the hydroxyl groups of 3,4-dephostatin on inhibition of PTP1B were studied. Elongation of the alkyl group newly formed an additional CH/π interaction with the deeper side of the active site of PTP1B. The two phenolic hydroxyl

Table 2. Inhibition of PTP1B by nitroso-free compounds

Compounds	IC_{50} ($\mu\text{g/mL}$)
20	47
22	2.9

groups formed a hydrogen bond network with polar functional groups of the side chains of PTP1B. Based on the structure–activity relationship study, novel nitroso-free PTPase inhibitors were designed and synthesized. The synthetic procedure was simple, and a variety of alkoxyamine compounds will be synthesized depending on the choice of alkoxyamine. Design, synthesis, and evaluation of PTPase inhibitory activity of further potent alkoxyamines having additional contact with PTP1B are under way.

Experimental

Melting points were determined using a Yanagimoto micro melting point apparatus and were uncorrected. IR spectra were measured with a Horiba FT-210 spectrophotometer. HRFAB-MS and FAB-MS were taken with a JEOL JMS-SX 102. NMR spectra were recorded with a JEOL JNM-EX-400 spectrometer. All reagents and solvents were purified by standard methods. All reactions were carried out under an argon atmosphere unless otherwise stated.

Synthesis of 3,4-dephostatin

3,4-Bis[(*tert*-butyldimethylsilyloxy)-*N*-methylaniline (4). To a solution of **3** (469 mg, 1.28 mmol) in 1.6 mL of MeOH was added 0.11 mL of formalin at 0°C, and the solution was stirred at the temperature for 30 min. Then, NaBH₃CN (80 mg, 1.28 mmol) was added portionwise to the reaction mixture at 0°C, and the solution was stirred for additional 3 h at room temperature. The solvent was evaporated after TLC confirmation of cessation of the reaction. The resulting residue was dissolved in CHCl₃, and the solution was washed with brine. The aqueous layer was back extracted with CHCl₃ twice. The combined organic layers were dried over Na₂SO₄ and concentrated in vacuo. The residue was purified by silica gel column chromatography by elution with EtOAc/*n*-hexane (1:40 to 1:10) to give 170 mg of **4** (0.463 mmol, 35% yield) as a colorless foam and recovered starting material **3** (0.194 mg, 0.548 mmol). The yield of **4** based on recovered **3** was 60%. The obtained starting material could be reused for the same reaction procedure. The physicochemical data of **4** were fully identical to the reported one.⁵ Requisite 3,4-dephostatin was afforded from **4** by the reported reaction scheme.⁵

Synthesis of 3,4-dephostatin analogs with elongated alkyl chain

Alkylation of compound 3. General procedure. Aldehyde and **3** were dissolved in MeOH. To the solution was added NaBH₃CN at 0°C, and the reaction mixture was stirred at room temperature. Then, the solution was evaporated, and the resulting residue was dissolved in EtOAc and washed with brine. The aqueous layer was extracted with EtOAc twice. The combined organic layer was dried over Na₂SO₄ and concentrated in vacuo. The residue was purified by silica gel column chromatography.

3,4-Bis[(*tert*-butyldimethylsilyloxy)-*N*-ethylaniline (5a). The reaction was conducted with 750 mg of **3** (2.15 mmol), 95 mg of acetaldehyde (2.15 mmol), and

135 mg of NaBH₃CN (2.15 mmol) in 2.5 mL of MeOH. The solution was stirred for 24 h. After purification (EtOAc/*n*-hexane 1:50), 589 mg of **5a** (1.54 mmol) was obtained as a colorless oil in 76% yield. IR (neat) ν_{\max} 2860, 1514, 1473, 1254, 1228, 839 cm⁻¹. ¹H NMR (400 MHz, CDCl₃) δ 6.65 (1H, d, *J*=8.3 Hz), 6.17 (1H, d, *J*=2.4 Hz), 6.11 (1H, dd, *J*=8.3, 2.4 Hz), 3.06, (2H, q, *J*=7.3 Hz), 1.22 (3H, t, *J*=7.3 Hz), 0.98 (9H, s), 0.97 (9H, s), 0.19 (6H, s), 0.15 (6H, s). ¹³C NMR (100 MHz, CDCl₃) δ 147.2, 143.3, 138.6, 121.6, 106.7, 106.0, 39.3, 26.0, 25.9, 18.5, 18.4, 15.0, -4.1, -4.2. HRFAB-MS (*m/z*) calcd for C₂₀H₃₉NO₂Si₂, 381.2519; found, 381.2500 (M⁺).

3,4-Bis[(*tert*-butyldimethylsilyloxy)-*N*-butylaniline (5b). The reaction was conducted with 738 mg of **3** (2.09 mmol), 184 mg of butyraldehyde (2.15 mmol), and 197 mg of NaBH₃CN (3.13 mmol) in 3.6 mL of THF. The solution was stirred for 14 h. After purification (EtOAc/*n*-hexane 1:50), 699 mg of **5b** (1.71 mmol) was obtained as a pale yellow oil in 82% yield. IR (neat) ν_{\max} 2858, 1614, 1514, 1254, 1228, 906, 841 cm⁻¹. ¹H NMR (400 MHz, CDCl₃) δ 6.65 (1H, d, *J*=8.8 Hz), 6.16 (1H, d, *J*=2.4 Hz), 6.10 (1H, dd, *J*=8.8, 2.4 Hz), 3.01, (2H, t, *J*=7.0 Hz), 1.57 (2H, m), 1.42 (2H, m), 0.99 (9H, s), 0.97 (9H, s), 0.95 (3H, t, *J*=7.3 Hz), 0.20 (6H, s), 0.15 (6H, s). ¹³C NMR (100 MHz, CDCl₃) δ 147.2, 143.4, 138.5, 121.6, 106.7, 106.0, 44.6, 31.8, 26.1, 26.0, 20.3, 18.5, 18.4, 13.9, -4.1, -4.2. HRFAB-MS (*m/z*) calcd for C₂₂H₄₃NO₂Si₂, 409.2832; found, 409.2856 (M⁺).

3,4-Bis[(*tert*-butyldimethylsilyloxy)-*N*-pentylaniline (5c). The reaction was conducted with 832 mg of **3** (2.35 mmol), 202 mg of valeraldehyde (2.35 mmol), and 222 mg of NaBH₃CN (3.52 mmol) in 4.5 mL of MeOH. The solution was stirred for 21 h. After purification (EtOAc/*n*-hexane 1:40), 737 mg of **5c** (1.74 mmol) was obtained as an orange oil in 74% yield. IR (neat) ν_{\max} 2858, 1514, 1254, 1225, 906, 839 cm⁻¹. ¹H NMR (400 MHz, CDCl₃) δ 6.65 (1H, d, *J*=8.3 Hz), 6.16 (1H, d, *J*=2.4 Hz), 6.10 (1H, dd, *J*=8.3, 2.4 Hz), 3.00, (2H, t, *J*=7.1 Hz), 1.59 (2H, m), 1.40–1.30 (4H, m), 0.98 (9H, s), 0.97 (9H, s), 0.91 (3H, t, *J*=7.1 Hz), 0.19 (6H, s), 0.15 (6H, s). ¹³C NMR (100 MHz, CDCl₃) δ 147.2, 143.4, 138.5, 121.6, 106.7, 106.0, 44.9, 29.4, 26.1, 26.0, 22.6, 18.5, 18.4, 14.1, -4.1, -4.2. HRFAB-MS (*m/z*) calcd for C₂₃H₄₅NO₂Si₂, 423.2989; found, 423.2966 (M⁺).

3,4-Bis[(*tert*-butyldimethylsilyloxy)-*N*-hexylaniline (5d). The reaction was conducted with 1.22 g of **3** (3.45 mmol), 351 mg of capronaldehyde (3.50 mmol), and 325 mg of NaBH₃CN (5.17 mmol) in 6 mL of MeOH. The solution was stirred for 24 h. After purification (EtOAc/*n*-hexane 1:50), 1.17 g of **5d** (2.67 mmol) was obtained as a colorless oil in 77% yield. IR (neat) ν_{\max} 2858, 1514, 1471, 1254, 1223, 906, 839, 779 cm⁻¹. ¹H NMR (400 MHz, CDCl₃) δ 6.65 (1H, d, *J*=8.3 Hz), 6.16 (1H, d, *J*=2.9 Hz), 6.10 (1H, dd, *J*=8.3, 2.4 Hz), 3.00, (2H, t, *J*=7.1 Hz), 1.62–1.55 (2H, m), 1.34–1.30 (6H, m), 0.98 (9H, s), 0.97 (9H, s), 0.90 (3H, t, *J*=7.1 Hz), 0.19 (6H, s), 0.15 (6H, s). ¹³C NMR (100 MHz, CDCl₃) δ 147.2, 143.4, 136.5, 121.5, 106.7, 106.0, 44.9, 31.7, 29.7, 26.9, 26.0, 22.6, 18.5, 18.4, 14.0, -4.1, -4.2. HRFAB-MS (*m/z*) calcd for C₂₄H₄₇NO₂Si₂, 437.3145; found, 437.3167 (M⁺).

Nitrosation of alkyl aniline compounds

General procedure. To a THF solution of **5** were added 1 N HCl and NaNO₂ at 0°C successively, the solution was then stirred at that temperature for 30 min. Next, THF was evaporated, and the resulting aqueous mixture was extracted with EtOAc three times. The combined organic layers were washed with brine, dried over Na₂SO₄, and concentrated in vacuo. The residue was purified by silica gel column chromatography.

3,4-Bis[(*tert*-butyldimethylsilyloxy]-*N*-ethyl-*N*-nitrosoaniline (6a**).** The reaction was conducted with 248 mg of **5a** (0.651 mmol), 2.6 mL of 1 N HCl, and 49.4 mg of NaNO₂ (0.716 mmol) in 13 mL of THF. After purification (EtOAc/*n*-hexane 1:10), 267 mg of **6a** (0.651 mmol) was obtained as a pale yellow oil in quantitative yield. IR (neat) ν_{\max} 2860, 1514, 1471, 1298, 1255, 901 cm⁻¹. ¹H NMR (400 MHz, CDCl₃) δ 7.05 (1H, d, *J*=2.4 Hz), 6.92 (1H, dd, *J*=8.3, 2.4 Hz), 6.89 (1H, d, *J*=8.3 Hz), 4.01, (2H, q, *J*=7.3 Hz), 1.15 (3H, t, *J*=7.3 Hz), 1.01 (9H, s), 1.00 (9H, s), 0.23 (6H, s), 0.22 (6H, s). ¹³C NMR (100 MHz, CDCl₃) δ 147.5, 146.6, 135.1, 121.2, 113.5, 112.9, 39.7, 25.9, 18.4, 11.7, -4.1. HRFAB-MS (*m/z*) calcd for C₂₀H₃₉N₂O₃Si₂, 411.2499; found, 411.2509 (MH⁺).

3,4-Bis[(*tert*-butyldimethylsilyloxy]-*N*-butyl-*N*-nitrosoaniline (6b**).** The reaction was conducted with 123 mg of **5b** (0.307 mmol), 2.6 mL of 1 N HCl, and 23.5 mg of NaNO₂ (0.341 mmol) in 14 mL of THF. After purification (EtOAc/*n*-hexane 1:50), 118 mg of **6b** (0.269 mmol) was obtained as a pale yellow oil in 87% yield. IR (neat) ν_{\max} 2860, 1514, 1471, 1255, 904, 840 cm⁻¹. ¹H NMR (400 MHz, CDCl₃) δ 7.04 (1H, d, *J*=2.4 Hz), 6.92 (1H, dd, *J*=8.8, 2.4 Hz), 6.89 (1H, d, *J*=8.8 Hz), 3.96, (2H, t, *J*=7.3 Hz), 1.51 (2H, m), 1.30 (2H, m), 1.00 (9H, s), 0.99 (9H, s), 0.90 (3H, t, *J*=7.3 Hz), 0.24 (6H, s), 0.23 (6H, s). ¹³C NMR (100 MHz, CDCl₃) δ 147.5, 146.6, 135.3, 121.1, 113.6, 113.0, 48.6, 44.2, 28.5, 25.9, 20.3, 18.4, 13.6, -4.1. HRFAB-MS (*m/z*) calcd for C₂₂H₄₃N₂O₃Si₂, 439.2812; found, 439.2785 (MH⁺).

3,4-Bis[(*tert*-butyldimethylsilyloxy]-*N*-pentyl-*N*-nitrosoaniline (6c**).** The reaction was conducted with 89.9 mg of **5c** (0.189 mmol), 1.5 mL of 1 N HCl, and 14.3 mg of NaNO₂ (0.207 mmol) in 9 mL of THF. After purification (EtOAc/*n*-hexane 1:3), 76.1 mg of **6c** (0.168 mmol) was obtained as an orange amorphous in 89% yield. IR (neat) ν_{\max} 2858, 1514, 1471, 1255, 1095, 903, 838 cm⁻¹. ¹H NMR (400 MHz, CDCl₃) δ 7.03 (1H, d, *J*=2.4 Hz), 6.92 (1H, dd, *J*=8.3, 2.4 Hz), 6.89 (1H, d, *J*=8.3 Hz), 3.95, (2H, t, *J*=7.5 Hz), 1.53 (2H, m), 1.35–1.22 (4H, m), 1.00 (9H, s), 0.99 (9H, s), 0.87 (3H, t, *J*=7.1 Hz), 0.22 (12H, s). ¹³C NMR (100 MHz, CDCl₃) δ 147.5, 146.6, 135.4, 121.2, 113.6, 113.0, 44.5, 29.2, 26.1, 25.9, 25.8, 22.2, 18.5, 13.8, -4.08, -4.13. HRFAB-MS (*m/z*) calcd for C₂₃H₄₅N₂O₃Si₂, 453.2969; found, 453.2975 (MH⁺).

3,4-Bis[(*tert*-butyldimethylsilyloxy]-*N*-hexyl-*N*-nitrosoaniline (6d**).** The reaction was conducted with 96.9 mg of **5d** (0.221 mmol), 2.3 mL of 1 N HCl, and 21.3 mg of NaNO₂ (0.309 mmol) in 15 mL of THF. After purification (EtOAc/*n*-hexane 1:10), 95.7 mg of **6d** (0.205 mmol) was

obtained as a pale yellow oil in 93% yield. IR (neat) ν_{\max} 2860, 1514, 1464, 1255, 902, 841, 783 cm⁻¹. ¹H NMR (400 MHz, CDCl₃) δ 7.03 (1H, d, *J*=1.4 Hz), 6.92 (1H, dd, *J*=8.8, 1.4 Hz), 6.89 (1H, d, *J*=8.8 Hz), 3.95, (2H, t, *J*=7.8 Hz), 1.53–1.47 (4H, m), 1.32–1.22 (4H, m), 1.00 (9H, s), 0.99 (9H, s), 0.86 (3H, t, *J*=7.3 Hz), 0.23 (6H, s), 0.22 (6H, s). ¹³C NMR (100 MHz, CDCl₃) δ 147.5, 146.6, 135.4, 121.2, 113.6, 113.1, 44.5, 31.3, 26.7, 26.4, 25.9, 22.5, 18.5, 14.0, -4.1. HRFAB-MS (*m/z*) calcd for C₂₄H₄₇N₂O₃Si₂, 467.3125; found, 467.3151 (MH⁺).

Final deprotection

General procedure. To a solution of nitrosated compound was added HF–NaF buffer (pH 4.73) at 0°C. The solution was stirred at room temperature. After confirming the disappearance of the substrate, THF was evaporated. The resulting mixture was diluted with brine and extracted with CHCl₃. The combined organic layers were dried over Na₂SO₄ and concentrated in vacuo. The residue was purified by silica gel column chromatography or preparative silica gel chromatography.

3,4-Dihydroxy-*N*-ethyl-*N*-nitrosoaniline (7a**).** The reaction was conducted with 2.30 g of **6a** (5.60 mmol) and 25 mL of buffer in 100 mL of THF for 20 h. After purification (EtOAc/*n*-hexane 4:1), 479 mg of **7a** (2.63 mmol) was obtained as a light brown powder in 47% yield: mp 124–126°C. IR (KBr) ν_{\max} 1604, 1533, 1463, 1248, 891 cm⁻¹. ¹H NMR (400 MHz, acetone-*d*₆) δ 8.23 (2H, br), 7.10 (1H, d, *J*=2.4 Hz), 6.95 (1H, d, *J*=8.8 Hz), 6.89 (1H, dd, *J*=8.8, 2.4 Hz), 4.01, (2H, q, *J*=7.3 Hz), 1.08 (3H, t, *J*=7.3 Hz). ¹³C NMR (100 MHz, acetone-*d*₆) δ 147.8, 145.7, 135.1, 116.3, 113.0, 109.3, 40.1, 11.9. HRFAB-MS (*m/z*) calcd for C₈H₁₁N₂O₃, 183.0770; found, 183.0792 (MH⁺).

3,4-Dihydroxy-*N*-butyl-*N*-nitrosoaniline (7b**).** The reaction was conducted with 104 mg of **6b** (0.237 mmol) and 1.8 mL of buffer in 4.2 mL of THF for 24 h. After purification (EtOAc/*n*-hexane 1:3 to 1:1), 28.1 mg of **7b** (0.134 mmol) was obtained as a gray powder in 56% yield: mp 100–102°C. IR (KBr) ν_{\max} 1618, 1537, 1467, 1271, 1174, 1101, 872, 795 cm⁻¹. ¹H NMR (400 MHz, CDCl₃) δ 9.71 (1H, br), 7.10 (1H, d, *J*=2.4 Hz), 6.98 (1H, d, *J*=8.8 Hz), 6.78 (1H, dd, *J*=8.8, 2.4 Hz), 5.89 (1H, br), 4.11, (2H, t, *J*=7.3 Hz), 1.59 (2H, m), 1.34 (2H, m), 0.92 (3H, t, *J*=7.3 Hz). ¹³C NMR (100 MHz, CDCl₃) δ 145.4, 145.0, 132.3, 114.5, 110.7, 107.9, 45.3, 28.3, 20.3, 13.5. HRFAB-MS (*m/z*) calcd for C₁₀H₁₅N₂O₃, 211.1083; found, 211.1091 (MH⁺).

3,4-Hydroxy-*N*-pentyl-*N*-nitrosoaniline (7c**).** The reaction was conducted with 75.0 mg of **7c** (0.166 mmol) and 1.3 mL of buffer in 3.5 mL of THF for 61 h. After purification (EtOAc/*n*-hexane 1:3), 20.6 mg of **7c** (91.7 μ mol) was obtained as a white powder in 55% yield: mp 101–103°C. IR (KBr) ν_{\max} 1616, 1535, 1209, 1176, 1105, 872, 794 cm⁻¹. ¹H NMR (400 MHz, CDCl₃) δ 7.46 (1H, d, *J*=2.9 Hz), 6.97 (1H, d, *J*=8.8 Hz), 6.80 (1H, dd, *J*=8.8, 2.9 Hz), 4.08, (2H, t, *J*=7.8 Hz), 1.60 (2H, m), 1.31 (4H, m), 0.88 (3H, t, *J*=6.8 Hz). ¹³C NMR (100 MHz, CDCl₃) δ 145.1, 144.9, 133.9, 114.6, 110.9, 107.9, 45.3, 29.1, 26.0,

22.2, 13.8. HRFAB-MS (m/z) calcd for $C_{11}H_{17}N_2O_3$, 225.1239; found, 225.1218 (MH^+).

3,4-Dihydroxy-*N*-hexyl-*N*-nitrosoaniline (7d). The reaction was conducted with 94.0 mg of **6d** (0.201 mmol) and 1.5 mL of buffer in 4.5 mL of THF. After purification (EtOAc/*n*-hexane 1:1), 23.8 mg of **7d** (94.3 μ mol) was obtained as a light brown powder in 47% yield: mp 104–106°C. IR (KBr) ν_{max} 1616, 1537, 1466, 1377, 1273, 1174, 1105, 871, 793 cm^{-1} . 1H NMR (400 MHz, $CDCl_3$) δ 7.47 (1H, d, $J=2.4$ Hz), 6.97 (1H, d, $J=8.8$ Hz), 6.89 (1H, dd, $J=8.8, 2.4$ Hz), 4.09 (2H, t, $J=7.8$ Hz), 1.65–1.55 (2H, m), 1.35–1.25 (6H, m), 0.87 (3H, t, $J=7.3$ Hz). ^{13}C NMR (100 MHz, $CDCl_3$) δ 145.3, 145.0, 133.7, 114.6, 110.8, 107.9, 45.5, 31.2, 26.7, 26.3, 22.4, 13.9. HRFAB-MS (m/z) calcd for $C_{12}H_{19}N_2O_3$, 239.1396; found, 239.1413 (MH^+).

Synthesis of methoxy derivatives

3-*tert*-Butyldimethylsilyloxy-4-methoxyaniline (11a). To a solution of 5.14 g of **8** (36.9 mmol) and 10.55 g of imidazole (155 mmol) in 120 mL of DMF was added 8.01 g of TBSCl (73.7 mmol) at 0°C. The solution was stirred for 5 h at room temperature. Then, brine was poured onto the solution, and the resulting mixture was extracted with toluene three times. The combined organic layers were dried over Na_2SO_4 and concentrated in vacuo. The residue was purified by silica gel column chromatography (EtOAc/*n*-hexane 1:6) to give 9.35 g of **11a** (36.9 mmol) as a colorless oil in quantitative yield. IR (neat) ν_{max} 1728, 1601, 1425, 1363, 1219, 1144, 1026 cm^{-1} . 1H NMR (400 MHz, $CDCl_3$) δ 6.68 (1H, d, $J=8.3$ Hz), 6.28 (1H, d, $J=2.9$ Hz), 6.25 (1H, dd, $J=8.3, 2.4$ Hz), 3.72 (3H, s), 3.37 (2H, br), 0.99 (9H, s), 0.15 (6H, s). ^{13}C NMR (100 MHz, $CDCl_3$) δ 146.0, 144.3, 140.6, 114.3, 109.5, 108.2, 56.6, 25.7, 18.4, –4.7. HRFAB-MS (m/z) calcd for $C_{13}H_{23}NO_2Si$, 253.1498; found, 253.1516 (M^+).

3-*tert*-Butyldimethylsilyloxy-4-methoxy-*N*-methylaniline (12a). To a solution of 1.79 g of **11a** (7.06 mmol) in 7.5 mL of DMF was added 0.64 mL of formalin (7.59 mmol) at 0°C. The solution was stirred for 30 min at 0°C. Then, 477 mg of $NaBH_3CN$ (7.59 mmol) was added to the solution, and the mixture was stirred for 3 h at room temperature. After confirmation of the cessation of the reaction, MeOH was evaporated, and the resulting mixture was extracted with EtOAc. The organic layer was washed with brine. The aqueous layer was extracted with EtOAc twice. The combined organic layers were dried over Na_2SO_4 and concentrated in vacuo. The residue was purified by silica gel column chromatography (EtOAc/*n*-hexane 1:15 to 1:5) to give 548 mg of **12a** (1.85 mmol) and 840 mg of unreacted substrate **11a** (3.14 mmol), the former obtained as a colorless foam in 30% yield (53% yield based on recovered **11a**). IR (neat) ν_{max} 1616, 1589, 1515, 1471 cm^{-1} . 1H NMR (400 MHz, $CDCl_3$) δ 6.74 (1H, d, $J=8.3$ Hz), 6.22 (1H, d, $J=2.9$ Hz), 6.19 (1H, dd, $J=8.3, 2.4$ Hz), 3.73 (3H, s), 2.78 (3H, s), 1.00 (9H, s), 0.16 (6H, s). ^{13}C NMR (100 MHz, $CDCl_3$) δ 146.3, 144.4, 143.5, 114.7, 106.9, 105.1, 56.8, 31.4, 25.7, 18.4, –4.7. HRFAB-MS (m/z) calcd for $C_{14}H_{25}NO_2Si$, 267.1655; found, 267.1649 (MH^+).

3-*tert*-Butyldimethylsilyloxy-4-methoxy-*N*-methyl-*N*-nitrosoaniline (13a). To a solution of 839 mg of **12a** (3.14 mmol) in 135 mL of THF were successively added 27 mL of 1N HCl and 237 mg of $NaNO_2$ (3.43 mmol) at 0°C. The solution was stirred for 30 min at 0°C. Then, THF was evaporated, and the resulting mixture was extracted with EtOAc three times. The combined organic layers were washed with brine, dried over Na_2SO_4 , and concentrated in vacuo. The residue was purified by silica gel column chromatography (EtOAc/*n*-hexane 1:10) to give 931 mg of **13a** (3.14 mmol) as a yellow powder in quantitative yield: mp 56–57°C. IR (KBr) ν_{max} 1593, 1515, 1425, 1267 cm^{-1} . 1H NMR (400 MHz, $CDCl_3$) δ 7.10 (1H, d, $J=2.9$ Hz), 7.02 (1H, dd, $J=8.8, 2.9$ Hz), 6.91 (1H, d, $J=8.8$ Hz), 3.85 (3H, s), 3.42 (3H, s), 1.01 (9H, s), 0.19 (6H, s). ^{13}C NMR (100 MHz, $CDCl_3$) δ 150.5, 145.7, 135.8, 113.0, 112.7, 112.0, 55.7, 32.0, 25.6, 18.4, –4.7. HRFAB-MS (m/z) calcd for $C_{14}H_{25}N_2O_3Si$, 297.1634; found, 297.1638 (MH^+).

3-Hydroxy-4-methoxy-*N*-methyl-*N*-nitrosoaniline (14a). To a solution of 305 mg of **13a** (1.03 mmol) in 20 mL of THF was added 3.9 mL of HF–NaF buffer (pH 4.73) at 0°C. The solution was stirred for 16 h at room temperature. Then, THF was evaporated, and the resulting mixture was extracted with EtOAc. The aqueous layer was extracted with EtOAc twice. The combined organic layers were washed with brine, dried over Na_2SO_4 , and concentrated in vacuo. The residue was purified by silica gel column chromatography (EtOAc/*n*-hexane 1:3) to give 188 mg of **14a** (1.03 mmol) as a yellow powder in quantitative yield: mp 108–109°C. IR (KBr) ν_{max} 1601, 1535, 1425, 1367, 1219, 1144, 1026 cm^{-1} . 1H NMR (400 MHz, $CDCl_3$) δ 7.14 (1H, d, $J=2.4$ Hz), 7.01 (1H, dd, $J=8.8, 2.4$ Hz), 6.92 (1H, d, $J=8.8$ Hz), 5.78 (1H, s), 3.95 (3H, s), 3.42 (3H, s). ^{13}C NMR (100 MHz, $CDCl_3$) δ 146.3, 146.0, 136.4, 111.2, 110.1, 106.8, 56.3, 32.0. HRFAB-MS (m/z) calcd for $C_8H_{11}N_2O_3$, 183.0770; found, 183.0772 (MH^+).

4-*tert*-Butyldimethylsilyloxy-3-methoxy-nitrobenzene (10). To a solution of 2.00 g of **9** (11.8 mmol) and 2.41 g of imidazole (35.4 mmol) in 50 mL of DMF was added 2.67 g of TBSCl (17.7 mmol) at 0°C. The solution was stirred for 19 h at room temperature. Then, brine was poured onto the solution, and the resulting mixture was extracted with toluene three times. The combined organic layers were dried over Na_2SO_4 and concentrated in vacuo. The residue was purified by silica gel column chromatography (EtOAc/*n*-hexane 1:40) to give 3.16 g of **10** (11.8 mmol) as a pale yellow powder in quantitative yield: mp 41–43°C. IR (KBr) ν_{max} 1585, 1508, 1466, 1352, 1298, 1233, 1097, 1026 cm^{-1} . 1H NMR (400 MHz, $CDCl_3$) δ 7.81 (1H, dd, $J=8.8, 2.9$ Hz), 7.74 (1H, d, $J=2.9$ Hz), 6.89 (1H, d, $J=8.8$ Hz), 3.89 (3H, s), 1.01 (9H, s), 0.20 (6H, s). ^{13}C NMR (100 MHz, $CDCl_3$) δ 151.5, 150.8, 142.1, 120.1, 117.6, 107.3, 55.7, 25.6, 18.5, –4.5. HRFAB-MS (m/z) calcd for $C_{13}H_{22}NO_4Si$, 284.1318; found, 284.1324 (MH^+).

4-*tert*-Butyldimethylsilyloxy-4-methoxyaniline (11b). To a solution of 3.12 g of **10** (11.7 mmol) was added 750 mg of 10% Pd/C and the mixture was stirred under H_2 atmosphere for 21 h at room temperature. Catalyst was filtered out through celite and the filtrate was concentrated in vacuo.

The residue was purified by silica gel column chromatography (EtOAc/*n*-hexane 1:4) to give 2.36 g of **11b** (9.31 mmol) as an amber powder in 80% yield: mp 39–40°C. IR (KBr) ν_{\max} 1632, 1593, 1514, 1236, 1169, 1122, 1032 cm^{-1} . ^1H NMR (400 MHz, CDCl_3) δ 6.65 (1H, d, $J=8.3$ Hz), 6.26 (1H, d, $J=2.4$ Hz), 6.16 (1H, dd, $J=8.3$, 2.9 Hz), 3.75 (3H, s), 3.42 (2H, br), 0.98 (9H, s), 0.12 (6H, s). ^{13}C NMR (100 MHz, CDCl_3) δ 151.4, 140.9, 137.6, 121.3, 107.0, 100.9, 53.4, 25.8, 18.4, –4.4. HRFAB-MS (m/z) calcd for $\text{C}_{13}\text{H}_{23}\text{NO}_2\text{Si}$, 253.1498; found, 253.1515 (M^+).

4-tert-Butyldimethylsilyloxy-3-methoxy-*N*-methylaniline (12b). To a solution of 2.34 g of **11b** (9.23 mmol) in 10 mL of MeOH was added 0.88 mL of formalin (9.23 mmol) at 0°C. The solution was stirred for 30 min at 0°C. Then, 659 mg of NaBH_3CN (10.5 mmol) was added to the solution, and the mixture was stirred for 2.5 h at room temperature. After confirmation of the cessation of the reaction, MeOH was evaporated, and the resulting mixture was extracted with EtOAc. The organic layer was washed with brine. The aqueous layer was extracted with EtOAc twice. The combined organic layers were dried over Na_2SO_4 and concentrated in vacuo. The residue was purified by silica gel column chromatography (EtOAc/*n*-hexane 1:10 to 1:3) to give 738 mg of **12b** (2.76 mmol) and 1.19 g of unreacted substrate **11b** (4.70 mmol), the former obtained as a colorless foam in 30% yield (61% yield based on recovered **11b**). IR (neat) ν_{\max} 1616, 1589, 1514, 1471, 1236, 1120, 1036 cm^{-1} . ^1H NMR (400 MHz, CDCl_3) δ 6.70 (1H, d, $J=8.3$ Hz), 6.19 (1H, d, $J=2.4$ Hz), 6.09 (1H, dd, $J=8.3$, 2.4 Hz), 3.77 (3H, s), 2.80 (3H, s), 0.98 (9H, s), 0.12 (6H, s). ^{13}C NMR (100 MHz, CDCl_3) δ 151.5, 144.6, 136.9, 121.2, 103.8, 98.5, 55.4, 31.4, 25.7, 18.4, –4.8. HRFAB-MS (m/z) calcd for $\text{C}_{14}\text{H}_{25}\text{NO}_2\text{Si}$, 267.1655; found, 267.1670 (M^+).

4-tert-Butyldimethylsilyloxy-3-methoxy-*N*-methyl-*N*-nitrosoaniline (13b). To a solution of 650 mg of **12b** (2.57 mmol) in 120 mL of THF were successively added 21 mL of 1 N HCl and 194 mg of NaNO_2 (2.81 mmol) at 0°C. The solution was stirred for 30 min at 0°C. Then, THF was evaporated, and the resulting mixture was extracted with EtOAc three times. The combined organic layers were washed with brine, dried over Na_2SO_4 , and concentrated in vacuo. The residue was purified by silica gel column chromatography (EtOAc/*n*-hexane 1:9) to give 590 mg of **13a** (1.99 mmol) as an orange oil in 77% yield. IR (neat) ν_{\max} 1594, 1514, 1471, 1392, 1342, 1280, 1255, 1180, 1124, 1090, 1034 cm^{-1} . ^1H NMR (400 MHz, CDCl_3) δ 7.18 (1H, d, $J=2.4$ Hz), 6.92 (1H, d, $J=8.3$ Hz), 6.85 (1H, dd, $J=8.3$, 2.4 Hz), 3.86 (3H, s), 3.44 (3H, s), 1.01 (9H, s), 0.19 (6H, s). ^{13}C NMR (100 MHz, CDCl_3) δ 151.5, 144.6, 136.5, 120.8, 111.3, 104.2, 55.5, 31.9, 25.6, 18.4, –4.7. HRFAB-MS (m/z) calcd for $\text{C}_{14}\text{H}_{25}\text{N}_2\text{O}_3\text{Si}$, 297.1634; found, 297.1635 (MH^+).

4-Hydroxy-3-methoxy-*N*-methyl-*N*-nitrosoaniline (14b). To a solution of 100 mg of **13b** (0.337 mmol) in 6 mL of THF was added 1.4 mL of HF–NaF buffer (pH 4.73) at 0°C. The solution was stirred for 14 h at room temperature. Then, THF was evaporated, and the resulting mixture was extracted with EtOAc. The aqueous layer was extracted with EtOAc twice. The combined organic layers were

washed with brine, dried over Na_2SO_4 , and concentrated in vacuo. The residue was purified by silica gel column chromatography (EtOAc/*n*-hexane 1:3) to give 61.4 mg of **14a** (0.337 mmol) as a yellow powder in quantitative yield: mp 42–44°C. IR (KBr) ν_{\max} 1618, 1516, 1259, 1122, 1093 cm^{-1} . ^1H NMR (400 MHz, CDCl_3) δ 7.21 (1H, d, $J=2.4$ Hz), 7.00 (1H, d, $J=8.8$ Hz), 6.92 (1H, dd, $J=8.8$, 2.4 Hz), 5.68 (1H, s), 3.95 (3H, s), 3.45 (3H, s). ^{13}C NMR (100 MHz, CDCl_3) δ 147.0, 145.2, 135.4, 114.4, 112.2, 103.4, 56.2, 32.2. HRFAB-MS (m/z) calcd for $\text{C}_8\text{H}_{11}\text{N}_2\text{O}_3$, 183.0770; found, 183.0776 (MH^+).

3,4-Dimethoxy-*N*-methyl-*N*-nitrosoaniline (16). To a solution of 635 mg of **15**⁴² (2.57 mmol) in 150 mL of THF were successively added 31 mL of 1 N HCl and 287 mg of NaNO_2 (4.16 mmol) at 0°C. The solution was stirred for 30 min at 0°C. Then, THF was evaporated, and the resulting mixture was extracted with EtOAc three times. The combined organic layers were washed with brine, dried over Na_2SO_4 , and concentrated in vacuo. The residue was purified by silica gel column chromatography (EtOAc/*n*-hexane 1:6) to give 711 mg of **16** (3.62 mmol) as a yellow powder in 95% yield: mp 83–84°C. IR (KBr) ν_{\max} 1597, 1518, 1471, 1280, 1255, 1234, 1180, 1040, 1022 cm^{-1} . ^1H NMR (400 MHz, CDCl_3) δ 7.22 (2H, d, $J=1.5$ Hz), 6.94 (1H, d, $J=1.5$ Hz), 3.93 (3H, s), 3.93 (3H, s), 3.45 (3H, s). ^{13}C NMR (100 MHz, CDCl_3) δ 149.6, 148.5, 135.9, 111.1, 111.1, 103.8, 56.1, 56.1, 31.9. HRFAB-MS (m/z) calcd for $\text{C}_9\text{H}_{13}\text{N}_2\text{O}_3$, 197.0926; found, 197.0931 (MH^+).

PTP1B inhibition assay

This PTP1B assay was carried out with *p*-nitrophenyl phosphate (pNPP) as the substrate in 96-well plates at 37°C. The assay mixture containing 5 μL of 40 mM NiCl_2 in H_2O , 5 μL of a bovine serum albumin solution (5 mg/mL in H_2O), 10 μL of PTP1B-agarose (Upstate Biotechnology, Lake Placid, NY), 53 μL of 50 mM Tris–HCl buffer (pH 7.0)/0.1 mM CaCl_2 , and 2 μL of various concentrations of inhibitor in assay buffer (50 mM Tris–HCl, 0.1 mM CaCl_2 , pH 7.0) (Upstate Biotechnology, Lake Placid, NY), was pre-incubated for 15 min. The enzyme reaction was started by the addition of 125 μL of pNPP solution (1.5 mg/mL in 50 mM Tris–HCl buffer). After 10 min incubation, the reaction was stopped by adding 20 μL of 13% (w/v) K_2HPO_4 solution, and the absorbance at 405 nm was then measured.

Molecular modeling study

Initial structures of PTP1B–ligand complexes were generated by superimposition of the ligand benzene ring and the benzene ring of phosphotyrosine reported from X-ray analysis of mutated PTP1B-phosphotyrosine-containing substrate.³² Coordinates of the nitroso and oxime moiety of the ligand were fixed on the plane of its benzene ring. The optimization was carried out by molecular mechanics energy minimization with program Insight II 99.0/Discover 3.0. The force-field parameters of CVFF were used, with coordinates of all heavy atoms of PTP1B fixed. CH/ π interactions were detected by the CHPI program as reported previously.⁴³

Synthesis of tetrazole compound

***N*-(3,4-Diacetoxyphenyl)-formamide (18).** To a solution of 1.20 mL of formic acid (32.0 mmol) in 60 mL of CH₂Cl₂ was added 2.74 g of 1-(3-dimethylaminopropyl)-3-ethylcarbodiimide hydrochloride (EDCI) (16.0 mmol) at 0°C, and the solution was stirred for 30 min at that temperature. Then, 2.76 mL of diisopropyl ethylamine (8.00 mmol) and a solution of 1.67 g of **17** (8.00 mmol) in 60 mL of CH₂Cl₂ were successively added to the reaction mixture at 0°C, and the solution was stirred for 4 h at room temperature. Brine was poured onto the solution and the aqueous layer was extracted with CHCl₃ twice. The combined organic layers were dried over Na₂SO₄ and concentrated in vacuo. The residue was purified by silica gel column chromatography (EtOAc/*n*-hexane 1:9) to give 1.43 g of **18** (6.03 mmol) as a colorless oil in 76% yield. This compound was obtained as a mixture of *cis*- and *trans*-isomers. IR (KBr) ν_{\max} 1772, 1745, 1697, 1685, 1541, 1525, 1427, 1234, 1195, 1168 cm⁻¹. ¹H NMR (400 MHz, CDCl₃) δ 8.60 (0.35H, d, *J*=11.2 Hz), 8.20 (0.35H, br), 8.16 (1H, d, *J*=1.5 Hz), 7.84 (1H, br), 7.58 (1H, d, *J*=2.4 Hz), 7.17 (1H, dd, *J*=8.8, 2.4 Hz), 7.14 (0.35H, d, *J*=1.5 Hz), 7.06 (1H, d, *J*=8.8 Hz), 6.93 (0.7H, m), 2.30 (2.1H, s), 2.29 (3H, s), 2.29 (2.1H, s), 2.28 (3H, s). ¹³C NMR (100 MHz, CDCl₃) δ 168.7, 168.5, 168.1, 162.3, 159.5, 159.3, 142.8, 142.0, 139.3, 138.3, 135.6, 135.2, 124.5, 123.5, 117.8, 116.9, 115.3, 114.3, 20.7, 20.6, 20.6, 20.4. HRFAB-MS (*m/z*) calcd for C₁₁H₁₂NO₅, 238.0715; found, 238.0712 (MH⁺).

3,4-Diacetoxybenzoisocyanide (19). To a solution of 70.0 mg of **18** (0.295 mmol) in 0.8 mL of CH₂Cl₂ were added 83.0 μ L of Et₃N (0.590 mmol) and 26.3 mg of triphosgene (90.4 μ mol) at 0°C. The solution was stirred for 3 h at room temperature. The precipitate was removed by passage through celite, and the filtrate was diluted with EtOAc. The organic layer was washed with brine, and the aqueous layer was extracted with EtOAc twice. The combined organic layers were washed with brine, dried over Na₂SO₄, and concentrated in vacuo. The residue was purified by silica gel column chromatography (EtOAc/*n*-hexane 1:2) to give 61.4 mg of **19** (0.225 mmol) as a yellow oil in 85% yield based on triphosgene. IR (neat) ν_{\max} 2129, 1776, 1500, 1371, 1201, 1171, 1041, 1012 cm⁻¹. ¹H NMR (400 MHz, CDCl₃) δ 7.30–7.22 (3H, m), 2.31 (3H, s), 2.30 (3H, s). ¹³C NMR (100 MHz, CDCl₃) δ 167.6, 167.6, 165.5, 142.9, 142.5, 124.7, 124.4, 122.0, 20.6, 20.5. HRFAB-MS (*m/z*) calcd for C₁₁H₁₀NO₄, 220.0610; found, 220.0604 (MH⁺).

3-(3,4-Dihydroxyphenyl)-tetrazole (20). A solution of 150 mg of **19** (1.11 mmol), 722 mg of NaN₃ (11.1 mmol) and 594 mg of NH₄Cl in 6 mL of DMF was stirred for 3 h at 80°C. The precipitate was removed by passage through celite, and the filtrate was concentrated in vacuo. Addition of Et₂O to the residue afforded a precipitate. The solid was washed with acetone and CHCl₃ to give 196 mg of **20** (1.10 mmol) as a brown powder in 99% yield: mp >300°C. IR (KBr) ν_{\max} 1616, 1527, 1489, 1346, 1306, 1213, 1107, 816 cm⁻¹. ¹H NMR (400 MHz, acetone-d₆) δ 9.53 (1H, s), 7.34 (1H, d, *J*=2.4 Hz), 7.21 (1H, dd, *J*=8.8, 2.4 Hz), 7.04 (1H, d, *J*=8.8 Hz). ¹³C NMR (100 MHz, acetone-d₆) δ 147.4, 147.9, 142.3, 127.7, 116.7, 110.0.

HRFAB-MS (*m/z*) calcd for C₉H₉N₄O₂, 179.0569; found, 179.0569 (MH⁺).

Synthesis of methoxime compound

***N*-Methoxy-3,4-dihydroxybenzaldimine (22).** To a solution of 275 mg of **21** (1.99 mmol) in 1.8 mL of EtOH–H₂O (2:1) were added 264 mg of sodium acetate and 183 mg of *O*-methylhydroxylamine hydrochloride, and the solution was stirred for 20 h at room temperature. Then, EtOH was evaporated, and the resulting mixture was extracted by CHCl₃ three times. The combined organic layers were dried over Na₂SO₄ and concentrated in vacuo. The residue was purified by silica gel column chromatography (EtOAc/*n*-hexane 2:1) to give 226 mg of **22** (1.35 mmol) as a yellow powder in 68% yield: mp 83–84°C. IR (KBr) ν_{\max} 1608, 1595, 1525, 1438, 1273, 1200, 1057, 820, 764 cm⁻¹. ¹H NMR (400 MHz, acetone-d₆) δ 7.95 (1H, s), 7.20 (1H, d, *J*=2.0 Hz), 6.98 (1H, dd, *J*=8.3, 2.0 Hz), 6.86 (1H, d, *J*=8.3 Hz), 5.61 (1H, br), 5.48 (1H, br), 3.94 (3H, s). ¹³C NMR (100 MHz, CDCl₃) δ 114.4, 145.7, 143.6, 125.2, 121.6, 115.4, 112.8, 61.8. HRFAB-MS (*m/z*) calcd for C₈H₁₀NO₃, 168.0661; found, 168.0663 (MH⁺) (Fig. 6).

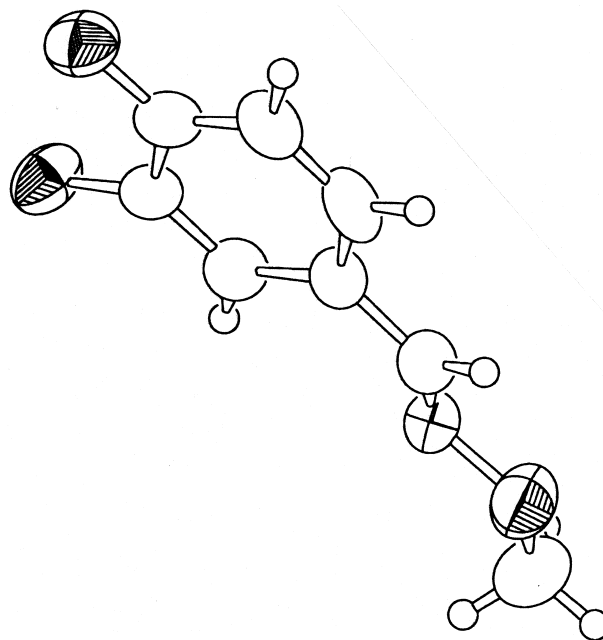


Figure 6. ORTEP drawing of crystal structure of **22**.

Acknowledgements

We thank Drs H. Naganawa and R. Sawa, Institute of Microbial Chemistry, for spectroscopic analysis, and Ms H. Nakamura, Institute of Microbial Chemistry, for X-ray crystallographic analysis. This work was financially supported in part by the Science Research Promotion Fund of the Promotion and Mutual Aid Corporation for Private Schools of Japan, and by the Special Coordination Funds for Promotions of Science and Technology from the Science and Technology Agency, Japan.

References

1. Tonks, N. K.; Neel, B. G. *Cell* **1996**, *87*, 365.
2. Imoto, M.; Kakeya, T.; Sawa, T.; Hayashi, C.; Hamada, M.; Takeuchi, T.; Umezawa, K. *J. Antibiot.* **1993**, *46*, 1342.
3. Kakeya, H.; Imoto, M.; Takahashi, Y.; Naganawa, H.; Takeuchi, T.; Umezawa, K. *J. Antibiot.* **1993**, *46*, 1716.
4. Watanabe, T.; Takeuchi, T.; Otsuka, M.; Umezawa, K. *J. Chem. Soc., Chem. Commun.* **1994**, 437.
5. Watanabe, T.; Takeuchi, T.; Otsuka, M.; Tanaka, S.; Umezawa, K. *J. Antibiot.* **1995**, *48*, 1460.
6. Umezawa, K. *Recent Res. Devel. Agric. Food Chem.* **1997**, *1*, 257.
7. Fujiwara, S.; Watanabe, T.; Nagatsu, T.; Gohda, J.; Imoto, M.; Umezawa, K. *Biochem. Biophys. Res. Commun.* **1997**, *238*, 213.
8. Lammers, R.; Bossenmaier, B.; Cool, D. E.; Tonks, N. K.; Schlessinger, J.; Fischer, E. H.; Ullrich, A. *J. Biol. Chem.* **1993**, *268*, 22 456.
9. Ahmad, F.; Azevedo, J. L.; Cortright, R.; Dohm, G. L.; Goldstein, B. J. *J. Clin. Invest.* **1997**, *100*, 449.
10. Hashimoto, N.; Feener, E. P.; Zang, W. R.; Goldstein, B. J. *J. Biol. Chem.* **1992**, *267*, 13 811.
11. Zang, W.-R.; Li, P.-M.; Oswald, M. A.; Goldstein, B. J. *Mol. Endocrinol.* **1996**, *10*, 575.
12. Elchembly, M.; Payette, P.; Michalliszyn, E.; Cromlish, W.; Collins, S.; Loy, A. L.; Normandin, D.; Cheng, A.; Himms-Hagen, J.; Chan, C. C.; Ramachandran, C.; Gresser, M. J.; Tremblay, M. L.; Kennedy, B. P. *Science* **1999**, *283*, 1544.
13. Burke Jr., T. R.; Kole, H. K.; Roller, P. P. *Biochem. Biophys. Res. Commun.* **1994**, *204*, 129.
14. Burke Jr., T. R.; Smyth, M. S.; Nomizu, M.; Otaka, A.; Roller, P. P. *J. Org. Chem.* **1993**, *58*, 1336.
15. Burke Jr., T. R.; Smyth, M. S.; Otaka, A.; Nomizu, M.; Roller, P. P.; Wolf, G.; Case, R.; Shoelson, S. E. *Biochemistry* **1994**, *33*, 6490.
16. Chen, L.; Wu, L.; Otaka, A.; Smyth, M. S.; Roller, P. P.; Burke Jr., T. R.; den Hertog, J.; Zhang, Z.-Y. *Biochem. Biophys. Res. Commun.* **1995**, *216*, 976.
17. Burke Jr., T. R.; Ye, B.; Yan, X.; Wang, S.; Jia, Z.; Chen, L.; Zhang, Z.-Y.; Barford, D. *Biochemistry* **1996**, *35*, 15 989.
18. Wang, Q.; Huang, Z.; Ramachandran, C.; Dinaut, A. N.; Taylor, S. D. *Bioorg. Med. Chem. Lett.* **1998**, *8*, 345.
19. Yokomatsu, T.; Murano, T.; Umesue, I.; Soeda, S.; Shimeno, H.; Shibuya, S. *Bioorg. Med. Chem. Lett.* **1999**, *9*, 529.
20. Burke Jr., T. R.; Ye, B.; Akamatsu, M.; Ford Jr., H.; Yan, X.; Kole, H. K.; Wolf, G.; Shoelson, S. E.; Roller, P. P. *J. Med. Chem.* **1996**, *39*, 1021.
21. Roller, P. P.; Wu, L.; Zhang, Z.-Y.; Burke Jr., T. R. *Bioorg. Med. Chem. Lett.* **1998**, *8*, 2149.
22. Hiriyanna, K. T.; Baedke, D.; Beak, K.-H.; Forney, B. A.; Kordiyak, G.; Ingebritsen, T. S. *Anal. Biochem.* **1994**, *223*, 51.
23. Cao, X.; Moran, E. J.; Siev, D.; Lio, A.; Ohashi, C.; Mjalli, A. M. M. *Bioorg. Med. Chem. Lett.* **1995**, *5*, 2953.
24. Burke Jr., T. R.; Yao, Z.-J.; Zhao, H.; Milne, G. W. A.; Wu, L.; Zhang, Z.-Y.; Voigt, J. H. *Tetrahedron* **1998**, *54*, 9981.
25. Wang, Q.; Dechert, U.; Jirik, F.; Withers, S. G. *Biochem. Biophys. Res. Commun.* **1994**, *200*, 577.
26. Arabaci, G.; Guo, X.-C.; Beebe, K. D.; Coggeshall, K. M.; Pei, D. *J. Am. Chem. Soc.* **1999**, *121*, 5085.
27. Hamaguchi, T.; Sudo, T.; Osada, H. *FEBS Lett.* **1995**, *372*, 54.
28. Miski, M.; Shen, X.; Cooper, R.; Gillum, A. M.; Fisher, D. K.; Miller, R. W.; Higgins, T. J. *Bioorg. Med. Chem. Lett.* **1995**, *5*, 1519.
29. Alvi, K. A.; Casey, A.; Nair, B. G. *J. Antibiot.* **1998**, *51*, 515.
30. Kagamizono, T.; Hamaguchi, T.; Ando, T.; Sugawara, K.; Adachi, T.; Osada, H. *J. Antibiot.* **1999**, *52*, 75.
31. Rice, R. L.; Rusnak, J. M.; Yokokawa, F.; Yokokawa, S.; Messner, D. J.; Boynton, A. L.; Wipf, P.; Lazo, J. S. *Biochemistry* **1997**, *36*, 15 965.
32. Puius, Y. A.; Zhao, Y.; Sullivan, M.; Lawrence, D. S.; Almo, S. C.; Zhang, Z.-Y. *Proc. Natl. Acad. Sci. U.S.A.* **1997**, *94*, 13 420.
33. Nishio, M.; Hirota, M. *Tetrahedron* **1989**, *45*, 7201.
34. Nishio, M.; Hirota, M.; Umezawa, Y. *The CH/π Interaction. Evidence, Nature, and Consequences*; Wiley: New York, 1998.
35. Yu, L.; McGill, A.; Ramirez, J.; Wang, P. G.; Zang, Z.-Y. *Biomed. Chem. Lett.* **1995**, *5*, 1003.
36. Sugawara, M.; Sasaki, A.; Yamaga, H.; Shinagawa, H.; Fukasawa, M.; Sumita, Y. EP 472,062, 1992; JP 212,102, 1990; *Chem. Abstr.* **1980**, *117* 7729.
37. Nishio, M.; Umezawa, Y.; Hirota, M.; Takeuchi, T. *Tetrahedron* **1995**, *51*, 8665.
38. Mascagna, D.; Ghanem, G.; Morandini, R.; D'Ischia, M.; Misuraca, G.; Lejeune, F.; Prota, G. *Melanoma Res.* **1992**, *2*, 25.
39. Eckert, H.; Forster, B. *Angew. Chem., Int. Ed. Engl.* **1987**, *26*, 894.
40. Fallon, F. G.; Herbst, R. M. *J. Org. Chem.* **1957**, *22*, 933.
41. Burankevich, J. V.; Love, A. M.; Volpp, G. P. *J. Org. Chem.* **1971**, *36*, 1.
42. Gangjee, A.; Zhu, Y.; Queener, S. F.; Francom, P.; Broom, A. D. *J. Med. Chem.* **1996**, *39*, 1836.
43. Umezawa, Y.; Nishio, M. *Bioorg. Med. Chem.* **1998**, *6*, 493.